Journal of Physics: Conference Series **488** (2014) 012035 doi:10.1088/1742-6596/488/1/012035

Transmission of highly charged ions through nanocapillaries of noncircular cross sections

HQ. Zhang[1, 2, a], N. Akram[1], I. L. Soroka[1], C. Trautmann[3], and R. Schuch[1, b]

[1]Physics Department, Stockholm University, S-10691 Stockholm, Sweden
[2]The School of Nuclear Science and Technology, Lanzhou University, Lanzhou, 730000, Gansu, China
[3]GSI Helmholtzzentrum Darmstadt, Germany

a: zhanghq02@gmail.com or zhanghq@lzu.edu.cn; b: schuch@fysik.su.se

Abstract. We report on effects from the geometrical shape of the guiding channels on the ion transmission profile. We find that capillaries of rhombic cross section produce rectangular shaped ion transmission profiles and, vice versa, capillaries of rectangular geometry give a rhombic beam shape. Our trajectory simulations for the incidence of 14-keV Ne^{7+} ions give clear evidence that the observed effect is due to the image forces experienced by the transmitting ions. They gain transverse energy due the image charge attraction towards the inner surfaces of the capillary. This leads to a defocusing of the ions leaving the capillaries. Due to the blocking of large deflection angles at the exit of the capillary, the transmitted ion beam is tailored into certain geometrical patterns.

1. Introduction

The transport of charged-particles through nanocapillaries has been focused for the past decade due to that the fabrication of membranes with nanosized capillaries in various materials and of various geometrical cross sections became possible [1-27]. It started with the discovery of the so-called "guiding effect" when transmitting ions through nanocapillaries in *polyethylene terephthalate* (PET) membranes [4]. It was found that the angular distributions of transmitted ions were centered around the direction of the capillary axes when the capillaries are tilted by an angle larger than that where they are geometrically transparent to the ion beam [4]. There is no significant energy loss or charge exchange in the bulk of the transmitted ions. Ions follow along the capillary and exit parallel to the channel orientation, independent of their entrance angles. This is of great interest for new ion-beam optics. The phenomenon is explained by the deposition of charges on the insulating capillary walls due to initial ion impact. Subsequent ions avoid close collisions and are then guided through the capillaries, in a manner similar to the channeling of particles in a crystal lattice potential. The formation of the guiding potential is, however, a time dependent process. A stationary stage of transmission is achieved after the charge deposition from incident ions and the draining of it through various discharge channels are in equilibrium. It has been found that a small number of charge patches, sequentially positioned on the capillary walls by the charging-up process, is guiding the ions through nanocapillaries [10-13].

The guiding effect is very effective with slow highly-charged ions (HCIs) and has been observed for millions of capillaries in various insulating materials such as in PET [4, 12-13, 22, 26], SiO_2 [8-11], Al_2O_3 [14-17], and polycarbonate (PC) [25-27] membranes. All previous studies on guiding of HCI

through insulating nanocapillaries have utilized capillaries of circular cross-sections. There the shape of the angular distribution of transmitted ions is only determined by the aspect ratio and the tilt angle of the capillaries with respect to the beam. We have revealed influences from the geometrical shape of the guiding channels on the ion transmission profile, when breaking the rotational symmetry with nanocapillaries of rhombic and rectangular cross sections [28-29]. It was found that the rhombic capillaries give a rectangular pattern and complementary, the rectangular capillaries produce a rhombic pattern [28].

In order to clarify the role of both the image force and the deposited charge in the beam tailoring effect, we measured the time evolution of the transmitted angular distributions during charge-up, starting with uncharged nanocapillaries. The starting phase of the angular distributions was recorded. The immediate onset of the tailored transmitted angular distribution as well as the trajectory simulations showed the dominant role of the image force, experienced instantaneously by the transmitting ions inside nanocapillaries. In this presentation, the role of the image charge in the tailoring of ion beams is discussed in more details. We show that the image force is deflecting the ion beam in the transverse direction and therefore leads to a defocusing. The larger deflection angles of the transmitted ions in the angular distributions correspond to the larger transverse energy gains of the transmitted ions due the image charge effect. At the exit of the capillary the transmitted ions with large deflection angles are blocked and this leads to the tailoring. This suggests defocusing of the ions by the image force also in the circular capillaries and sheds light on the broadening of the angular distributions, seen earlier in the guiding effect [4, 7, 9, 12, 13, 16, 26].

2. Sample preparations and experiments

Membranes with nanocapillaries were prepared by exposing 20-µm thick muscovite and 10-µm thick phlogopite mica wafers to 2.3-GeV Pb and 1.4-GeV Xe ions, respectively. The irradiation was performed under normal beam incidence at the linear accelerator UNILAC of the GSI Helmholtz Centre applying a fluence of 5×10^7 ions/cm^2. The projectiles pass through the entire thickness of the samples and produce latent tracks of few nanometers in diameter [30]. The irradiated samples were then etched at room temperature in a 20% aqueous solution of hydrofluoric acid, the muscovite for 10 minutes and the phlogopite mica for 3 minutes. In contrast to round shaped channels in isotropic polymers, the crystal-orientation dependent etching rates lead to a rhombic cross section in muscovite mica and a rectangular cross section in phlogopite mica with the axes of all nanocapillaries being aligned along the same orientation as shown by scanning electron microscopy (SEM) (figure 1).

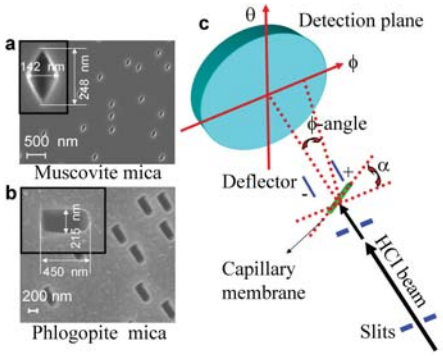

Figure 1 (color online). SEM images of track-etched mica membranes with nanocapillaries of (**a**) rhombic and (**b**) rectangular cross sections and (**c**) a schematic view of the setup for the ion transmission experiments.

The rhombic channels in muscovite mica have acute angles of 60° and obtuse angles of 120° with a long axis of 248 nm and a short axis of 142 nm, and the channel length of 20 µm gives the geometrical opening angle of 0.4° for the short axis. The rectangular capillaries have dimension of 450 nm by 215

nm corresponding to a porosity of 4.8 %. The membrane thickness of 10 µm results in a geometrical opening angle of 1.23° along the short sides. The area density (determined by the applied ion fluence) together with the cross section of the capillaries yields a geometrical transparency (porosity) of 0.9 % and 4.8 % for rhombic and rectangular capillaries, respectively. The geometrical transparencies of these capillaries are sufficiently so low that the nanochannels can be regarded as individually well-separated objects. To avoid macroscopic charge-up, the both sides of the capillary membrane were coated with 10 nm-thick layers of Au.

The transmission experiments with HCI were performed at the ECR ion source and S-EBIT of Stockholm University. Beams of Ne^{7+} ions were collimated to a divergence of less than 0.2°, size of 2×2 mm^2, and intensity of 8 to 80 pA/mm^2 at the membrane position by a pair of four-jaw slits, set 1.55 m apart. The capillary membrane was mounted on a goniometer of five-degree adjustments: three in translational directions and two in rotational directions. The capillaries can be oriented in the direction of the incident beam by the tilt angle α. The observation angles ϕ and θ, related to the hit position in the detection plane, are given with respect to the incident beam direction (see figure 1). The transmitted ions were imaged using two-dimensional micro-channel plates (MCPs) with a resistive anode [31]. An electrostatic deflector was mounted downstream of the capillary membrane to analyze the charge states of the transmitted ions (figure 1).

3. Ion transmission results

The angular distributions of 7-keV Ne^{7+} ions transmitted through the rhombic and rectangular capillaries, with a tilt angle α = 0°±0.25°, are shown in figure 2. We find that the rectangular capillaries give a rhombic angular distribution of transmitted ions, with the long axis of the rhombus parallel to the short sides of the rectangles (figure 2a), and orthogonally, rhombic capillaries produce a rectangular transmitted angular profile with the long axes of the rhombi parallel to the short side of the rectangle (figure 2b) [28]. This gives strong evidence that the angular distribution does not originate from the shape of the primary beam. Also, it has been found that only the ionic portion of the transmitted beam is tailored by the interaction with the capillary wall [28].

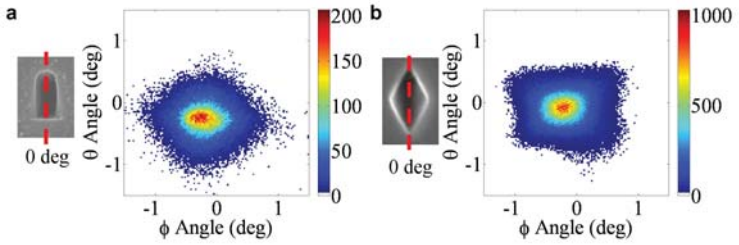

Figure 2 (color online). Two-dimensional angular distributions for 7-keV Ne^{7+} transmitted through mica capillaries of rectangular (**a**) and rhombic (**b**) cross-section with the corresponding orientations of the long sides of the rectangles and the long axes of the rhombi in a plane perpendicular to the beam (as indicated on the left panel).

In the search for the origin of this phenomenon, we consider three possibilities: (1) due to the Coulomb repulsion force directly from the deposited charge on the walls, (2) the force from the exit field due to the deposition of charges close to the entrances of millions of capillaries [6], and (3) due to the force from the induced image charge by the projectiles. In case (3) the interaction between the ions and walls is expected to be instantaneous while the other two cases it is dependent on the deposited charge and thus dependent on the charge-up time. In order to identify the role of these forces, we measured the time evolution of the transmitted angular distribution at α = -0.1° for the incidence of 14-keV Ne^{7+}, starting with uncharged capillaries (α = -0.1° was experimentally determined by the offset of the centroid position of the transmitted angular distribution from the peak center of the primary beam [29]). In this measurement the angular distributions at the very early stage of

transmission was recorded. Figure 3a shows the transmission angular profile after, on average, 4 ions have entered a single capillary. The characteristic shapes appearing for such a low number of ions gives evidence that the ion transmission profile is tailored by the image forces (3) rather than case (1) and (2).

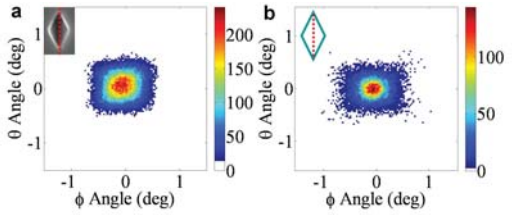

Figure 3 (color online). Initial angular distribution of the transmitted ions is shown for Ne^{7+} at the incident energy of 14 keV: experimental profiles with $\alpha = -0.1°$ in (**a**); simulated transmission profiles considering the image force effect for rhombic capillaries in (**b**). Insets in the upper left corners of each graph show the orientations of the rhombi.

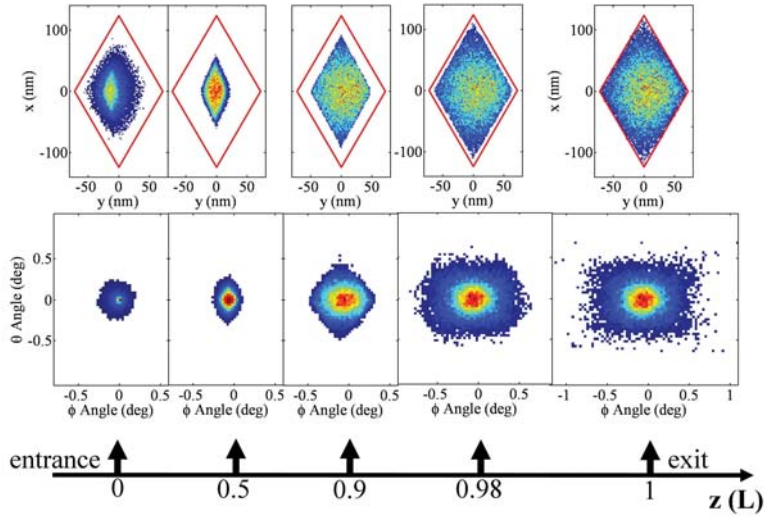

Figure 4 (color online). Simulated results: (Top) The ion flux distributions in the transverse plane at various distances from the entrance along the axis of the rhombic capillary z for $\alpha = -0.1°$ (with channel length L), and (Bottom) the corresponding angular distributions of the transmitted ions in the detection plane for 14-keV Ne^{7+} ions.

We performed a trajectory simulation to obtain the transmitted angular distribution, by considering a simplified image forces (a superposition of the image forces from each side of the nanocapillary wall) [28-29, 31]. The injection angles of the ions and the beam divergence are taken from the experiments. The incident kinetic energy of the beam is fixed at 14 keV. As seen in figure 3b, the experimental transmission profile is reproduced quite well by the simulation.

To demonstrate how the image force tailors the ion beam, we plot the ion flux distribution in the transverse plane at various distances, z, from the entrance along the axis of the rhombic capillary and the corresponding angular distribution, which is expected to be seen in the detection plane, in figure 4. Our calculations reveal that the angular distribution of the ion beam, initially with a circular shape at the entrance, becomes rhombic at a distance $z \approx 0.5\ L$, and then it starts to expand. Close to the exit of the capillary the charged particles with the largest deflection angles are blocked off, thus, creating the observed angular distributions.

The projectiles gain transverse energy due to the image charge attraction and therefore their kinetic energy increases a bit from the incident energy (14000 eV). In figure 5a we show the simulated kinetic

energy distributions of the ions at various distances, z, from the entrance along the axis of the rhombic capillary. It can be seen that the projectiles gain more transverse energies with increasing distance from the entrance of the capillary. We plot in figure 5b also the yields of the transmitted ions as a function of the kinetic energy (E) in intervals: E < 14000.4 eV, 14000.4 eV < E < 14001.5 eV and E > 14001.5 and the corresponding angular distributions at the exit of the capillary in figure 5c, 5d and 5e. It can be seen that the tailored part is less than 10 % in the transmitted angular distributions.

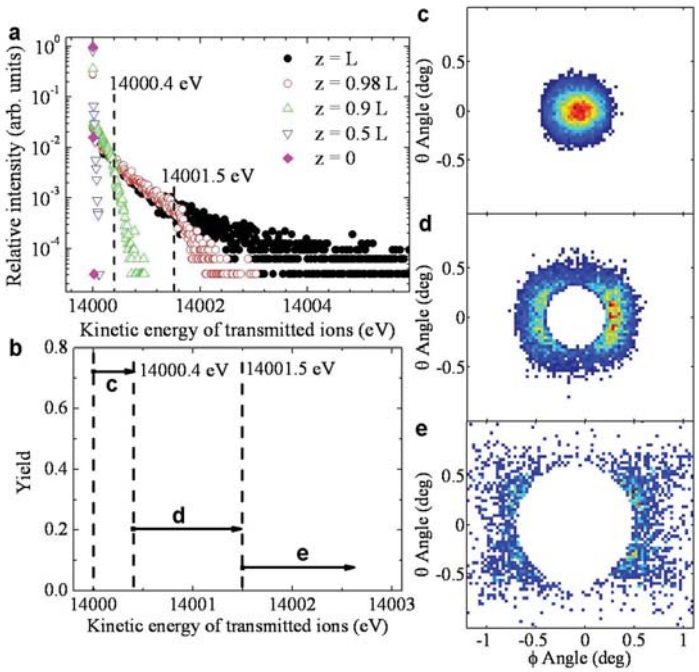

Figure 5 (color online). (**a**) The simulated kinetic energy distributions of the projectiles for the incident energy of 14000 eV, due to the image charge deflection in the transverse direction, at various distances from the entrance along the axis of the rhombic capillary z (with channel length L); (**b**) the yield of the transmitted ions as a function of the kinetic energy in intervals (E < 14000.4 eV, 14000.4 eV < E < 14001.5 eV and E > 14001.5) at the exit ($z = L$) of the capillary; the corresponding angular distributions of the transmitted ions were plotted in (**c**), (**d**) and (**e**), as denoted in (**b**) for the incidence of 14-keV Ne^{7+} ions at a tilt angle of $\alpha = -0.1°$.

4. Conclusions and outlook

Our results demonstrate that the shape of ion beams can be tailored by transmission through nanocapillaries of defined geometrical cross sections. The immediate onset of the characteristic shape in the transmitted angular distributions from the time evolution measurement, starting with uncharged capillaries, as well as trajectory simulations show clear evidence that the tailoring effect is attributed to the image forces induced when the projectiles transmit through the nanochannels. The image force deflects ions in the transverse direction and therefore defocuses the transmitted beam which, together with the collimation at the exit of the capillary for large deflection angles of the transmitted ions, results in the tailoring effect.

Our findings suggest exploitation of capillaries of various conductivities and cross sections as a tool to guide, focus, as well as shape, ion beams for diverse applications. With future developments of nanostructure engineering it should be possible to produce membranes with capillaries of any designed shape. The tailored particle beams can be used, for example in microprobes, for ion beam writing and structured ion implantation.

References

[1] Martin C R 1994 *Science* **266** 1961
[2] Ninomiya S, Yamazaki Y, Koike F, Masuda H, Azuma T, Komaki K, Kuroki K, and Sekiguchi M 1997 *Phys. Rev. Lett.* **78** 4557
[3] Tökési K, Wirtz L, Lemell C and Burgdörfer J 2000 *Phys. Rev. A* **61** 020901
[4] Stolterfoht N, Bremer J H, Hoffmann V, Hellhammer R, Fink D, Petrov A and Sulik B 2002 *Phys. Rev. Lett.* **88** 133201
[5] Schiessl K, Palfinger W, Tökési K, Nowotny H, Lemell C and Burgdörfe J 2005 *Phys. Rev. A* **72** 062902
[6] Schiessl K, Tökési K, Solleder B, Lemell C, and Burgdörfe J 2009 *Phys. Rev. Lett.* **102** 163201
[7] Víkor Gy, Rajendra Kumar R T, Pešič Z D, Stolterfoht N, and Schuch R 2005 *Nucl. Instr. Meth. Res. B* **233** 218
[8] Rajendra Kumar R T, Badel X, Víkor Gy, Linnros J, and Schuch R 2005 *Nanotechnology* **16** 1697
[9] Sahana M B, Skog P, Víkor Gy, Rajendra Kumar R T, and Schuch R 2006 Phys. Rev. A **73** (4) 040901(R)
[10] Skog P, Zhang HQ and Schuch R 2008 *Phys. Rev. Lett.* **101** 223202
[11] Zhang H Q, Skog P and Schuch R 2010 *Phys. Rev. A* **82** 052901
[12] Kanai Y, Hoshino M, Kambara T, Ikeda T, Hellhammer R, Stolterfoht N, and Yamazaki Y 2009 *Phys. Rev. A* **79** 012711
[13] Stolterfoht N, Hellhammer R, Fink D, Sulik B, Juhász Z, Bodewits E, Dang H M, and Hoekstra R 2009 *Phys. Rev. A* **79** 022901
[14] Mátéfi-Tempfli S, Mátéfi-Tempfli M, Piraux L, Juhász Z, Biri S, Fekete É, Iván I, Gáll F, Sulik B, Víkor Gy, Pálinkás J and Stolterfoht N 2006 *Nanotechnology* **17** 3915
[15] Krause H F, Vane C R, and Meyer F W 2007 *Phys. Rev. A* **75** 042901
[16] Skog P, Soroka I L, Johansson A, and Schuch R 2007 *Nucl. Instrum. Methods B* **258** 145
[17] Juhász Z *et al* 2009 *Nucl. Instrum. Methods B* **267** 321
[18] Ikeda T, Kanai Y, Kojima T M, Iwai Y, Kambara T, Yamazaki Y, Hoshino M, Nebiki T, and Narusawa T 2006 *Appl. Phys. Lett.* **89** 163502
[19] Cassimi A *et al* 2008 *Int. J. Nanotechnol.* **5** 809
[20] Cassimi A *et al* 2009 *Nucl. Instrum. Methods B* **267** 674
[21] Iwai Y *et al* 2008 *Appl. Phys. Lett.* **92** 023509
[22] Juhász Z, Sulik B, Rácz R, Biri S, Bereczky R J, Tökési K, Köver A, Pálinkás J, and Stolterfoht N 2010 *Phys. Rev. A* **82** 062903
[23] Das S, Dassanayake B S, Winkworth M, Baran J L, Stolterfoht N, and Tanis J A 2007 *Phys. Rev. A* **76** 042716
[24] Sun G *et al* 2009 *Phys. Rev. A* **79** 052902 ; Chen L *et al* 2011 *Phys. Rev. A* **84** 032901
[25] Li D, Wang Y, Zhao Y, Xiao G, Zhao D, Xu Z and Li F 2009 *Nucl. Instrum. Methods B* **267** 469
[26] Stolterfoht N, Hellhammer R, Juhász Z, Sulik B, Bayer V, Trautmann C, Bodewits E, de Nijs A J, Dang H M, and Hoekstra R 2009 *Phys. Rev. A* **79** 042902
[27] Stolterfoht N, Hellhammer R, Sulik B, Juhász Z, Bayer V, Trautmann C, Bodewits E and Hoekstra R 2011 *Phys. Rev. A* **83** 062901
[28] Zhang H -Q, Akram N, Skog P, Soroka I L, Trautmann C and Schuch R 2012 *Phys. Rev. Lett.* **108** 193202
[29] Zhang H -Q, N. Akram, Soroka I L, Trautmann C and Schuch R 2012 *Phys. Rev. A.* **86** 022901
[30] Ackermann J, Angert N, Neumann R, Trautmann C, Dischner M, Hagen T, and Sedlacek M 1996 *Nucl. Instrum. Methods B* **107** 181
[31] Zhang H, Ph.D. Thesis, Stockholm University, Stockholm, 2010